

# A Solvation/Desolvation Indicator based on van der Waals Interactions between Solvent and Porphyrins

Akiharu Satake,<sup>\*,[a],[b]</sup> Yuki Suzuki,<sup>[a]</sup> Motonobu Sugimoto,<sup>[a]</sup> Tatsumi Shimazaki,<sup>[a]</sup> Hidekazu Ishii,<sup>[b]</sup> Yusuke Kuramochi<sup>[a],[b]</sup>

**Abstract:** Solvation is a ubiquitous phenomenon associated with molecules in solutions. It often determines the equilibria of molecular systems and the rates of chemical reactions. Van der Waals interaction (a general term) includes weak interactions among noncharged compounds and it contributes significantly to solvation. We report on the distinct observation of van der Waals interaction between solvent and porphyrin derivatives. Bis(imidazolylporphyrinatozinc) structures connected through a 1,3-butadiyne moiety give two types of coordination polymers, **E** (extended) and **S** (stacked) polymers, exclusively. **E** polymers have larger solvent-accessible surface areas than the corresponding **S** polymers. Therefore, **E** polymers are better solvated than **S** polymers, providing an indicator of solvation and desolvation for the solvents used. A simple method (like a litmus test) was developed to evaluate the solvation ability of various solvents. Sixty-seven solvents and liquid compounds were tested, under the same conditions, using a conventional UV-Vis spectrometer. The results revealed a new liquid group with high solvation ability towards the porphyrins, and clarified van der Waals interaction assisted by secondary interaction on the substituents. The indicator system should contribute to the solution chemistry of molecules and materials, and to supramolecular chemistry interactions among hetero components.

## Introduction

Solvation is a ubiquitous phenomenon associated with molecules in solutions. Equilibria of molecular systems<sup>[1]</sup>, conformational changes<sup>[2]</sup>, dispersion of carbon material<sup>[3]</sup>, selectivity in chemical reactions<sup>[4]</sup>, and rates of chemical reactions<sup>[5]</sup> are often determined by the solvents used in systems. In these cases, solvation of the molecules or solutes plays a key role. Van der Waals interaction (a general term) includes weak interactions among noncharged compounds and it contributes significantly to solvation. However, its distinct observation in solution is difficult; to date, it has generally been observed as chemical and physicochemical phenomena<sup>[6]</sup>, including other interactions and bulk solvent effects, as all-in<sup>[7]</sup>. Here, we report on the distinct observation of van der Waals

interaction between solvent and porphyrin derivatives, which are derivatives of noncharged and nonpolar large  $\pi$ -conjugated compounds. Because solvent-solute interaction occurs in many-body interactions, including other solvent-solvent and solute-solute interactions, the method is able to evaluate not only solvation but also desolvation of various solvents simultaneously. In related works, the formation of supramolecules in various solvents was studied<sup>[8]</sup>; however, applicable solvents were limited because supramolecules either did not form or were insoluble. Following the present assessment system, 67 solvents and liquid compounds were tested, all under the same conditions, using a conventional UV-Vis spectrometer. The method is quite simple and responsive (like a litmus test). The results revealed a new liquid group with high solvation ability towards the porphyrins, and clarified van der Waals interaction assisted by secondary interaction on the substituents. Van der Waals interaction works specifically and anisotropically between solvent molecules and porphyrin solutes. The indicator system should contribute to the solution chemistry of molecules and materials, and to supramolecular chemistry interactions among hetero components<sup>[9]</sup>.

## Results and Discussion

### Design and Characterization of **E** and **S** polymers.

We have previously reported interconversion systems between two types of coordination dimers<sup>[10]</sup>, **E** (extended) and **S** (stacked) dimers, composed of two monoimidazolylbisporphyrinatozinc complexes. They are coordination isomers connected by two types of strong, but labile, complementary coordination bonds. In efforts to develop a solvation and desolvation indicator, the above discrete system was extended to infinite supramolecular polymer systems between **E** and **S** polymers, as shown in Figure 1.

The both **E** and **S** polymers are considered to be constructed by complementary coordination bonds of an imidazole to a zinc ion interaction, in which only a five-coordinating complex is stable. Under highly diluted conditions, other non-complementary coordination and non-specific interactions are eliminated. Therefore, formation of only the two types of supramolecular polymers is expected.

The motion between **E** and **S** polymers is similar to folding and spreading playing cards. **E** polymers have larger solvent-accessible surface areas than the corresponding **S** polymers. Therefore, **E** polymers are expected to be better solvated than **S** polymers, providing an indicator of solvation and desolvation for the solvents used. It is also expected that sensitivity towards external conditions increases in the cooperative polymer formation. Unit molecules for the polymer system, **1Zn<sub>2</sub>** and **2Zn<sub>2</sub>**, were prepared (see Figure 2 and Supplementary Information).

[a] Prof. A. Satake, Mr. Y. Suzuki, Mr. M. Sugimoto, Mr. T. Shimazaki, Dr. Y. Kuramochi  
Graduate School of Science  
Tokyo University of Science  
1-3 Kagurazaka, Shinjuku-ku, Tokyo 162-8601, Japan  
E-mail: satake@rs.kagu.tus.ac.jp

[b] Mr. H. Ishii  
Department of Chemistry, Faculty of Science Division II,  
Tokyo University of Science

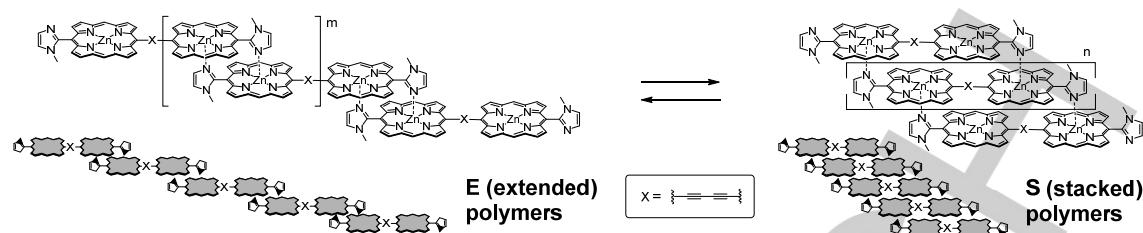


**Figure 1.** **S** (stacked) and **E** (extended) polymers constructed from bis(imidazolylporphyrinatozinc) molecules. **E** polymers have larger solvent-accessible surface areas, expecting higher solvation.

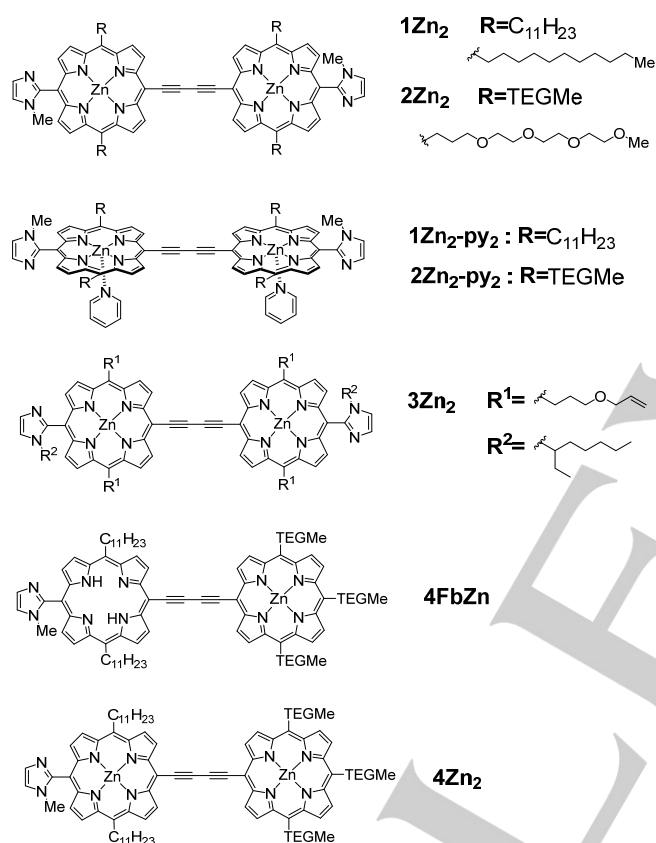


**Figure 2.** Structures of porphyrin derivatives.

They were bis(imidazolylporphyrinatozinc) structures connected through a 1,3-butadiyne moiety, to which the substituent groups, hydrophobic undecyl ( $C_{11}H_{23}$ ) and hydrophilic triethylene glycol methyl ether (TEGMe), were attached in **1Zn<sub>2</sub>** and **2Zn<sub>2</sub>**, respectively. The introduction of different types of side chains is helpful in the discussion of secondary interaction on the substituents and the main van der Waals interaction on the porphyrin frames.

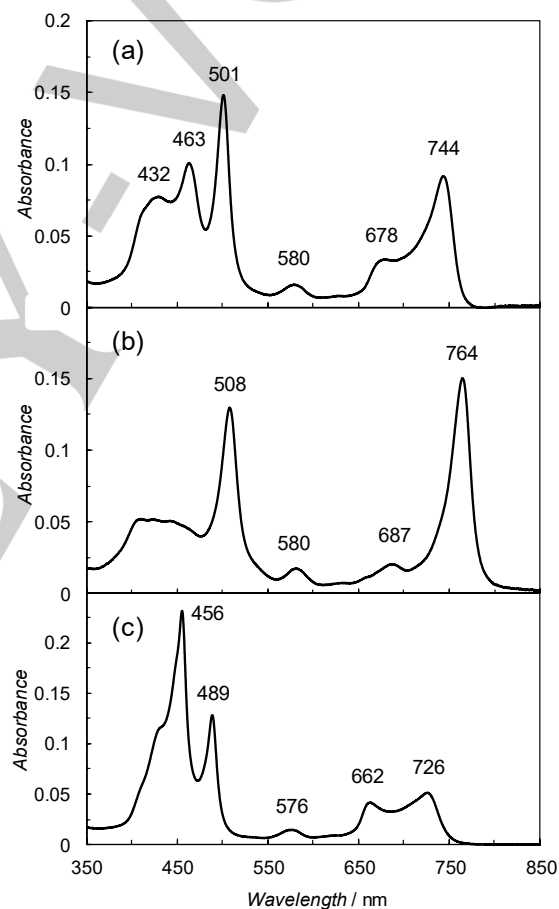


**Figure 3.** UV-vis spectra of **1Zn<sub>2</sub>** ( $2.5 \times 10^{-6}$  M) in (a)  $CHCl_3$  (b) 2-propanol (c) pyridine. Characteristic peaks are 432, 463, 501, and 744 nm in (a), 508 and 764 nm in (b), and 456, 489, 662, and 726 nm in (c).

In preliminary investigations, solvents affording **E** or **S** polymers were studied based on their UV-Vis absorption spectra. A spectral shape of the **E** polymer could be predicted by referring to that of **3Zn<sub>2</sub>**, reported previously<sup>[11]</sup>. On the other hand, UV-Vis spectra of **S** polymers are unknown. We were nonetheless confident that these spectra could be distinguished

from those of the **E** polymers because, on basis of the molecular model, the structure of **S** polymers must be restricted to be a coplanar conformation. A UV-Vis spectrum of **1Zn<sub>2</sub>** in chloroform ( $2.5 \times 10^{-6}$  M) is shown in Figure 3a. The peak in the longest wavelength region was observed at  $\lambda_{\text{max}}$  744 nm. The spectral shape and the  $\lambda_{\text{max}}$  value of **1Zn<sub>2</sub>** are similar to those of bisporphyrin **3Zn<sub>2</sub>**. In the  $^1\text{H}$  NMR spectrum of **1Zn<sub>2</sub>** in  $\text{CDCl}_3$ , four characteristic  $\beta$ -protons of the **E** polymer were observed at 10.38, 9.88, 8.97, and 5.61 ppm, respectively (Figures S1 and S2). Both sets of analytical data indicate that the structure of **1Zn<sub>2</sub>** obtained in chloroform is **E** polymer. On the other hand, a UV-Vis spectrum of **1Zn<sub>2</sub>** in 2-propanol ( $2.5 \times 10^{-6}$  M) was entirely different (see Figure 3b). The longest wavelength peak was sharpened and red-shifted to 764 nm. In the Soret band region (400–550 nm), the maximum peak was shifted from 501 to 508 nm, and the intensities of the peaks at 432 and 463 nm became small.

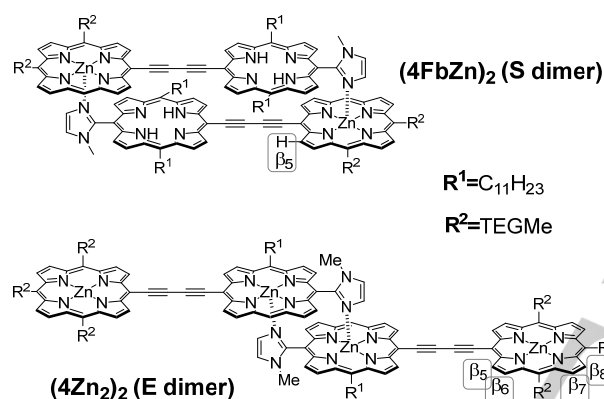


**Figure 4.** Structures of complementary coordination dimers of **4FbZn** and **4Zn<sub>2</sub>**.

The spectral change indicated drastic conformational change from the **E** polymer of **1Zn<sub>2</sub>**. As a reference, a UV-Vis spectrum of the dissociated monomeric structure of **1Zn<sub>2</sub>-py<sub>2</sub>** in pyridine is shown in Figure 3c. Increased intensity of the peak at 456 nm indicates increasing orthogonal conformation of **1Zn<sub>2</sub>** between the two porphyrin planes<sup>[12]</sup>. The spectral change observed in Figure 3b is similar to that of 1,3-butadiyne-connected bisporphyrins having coplanar conformation<sup>[13]</sup>, suggesting that **S** polymers of **1Zn<sub>2</sub>** are formed in 2-propanol.

As another reference for the UV-vis spectra, two bisporphyrins connected through a 1,3-butadiyne moiety, **4FbZn** and **4Zn<sub>2</sub>** were prepared (see Figure 2 and Supplementary Information). Since they have only one imidazolyl group, complementary coordination dimers are expected to be formed as shown in Figure 4. Their  $^1\text{H}$  NMR spectra in  $\text{CDCl}_3$  and the assignments of the  $\beta$  protons are shown in Figures S3–S6. As expected, **4FbZn** gave only **S** dimer, because it had one zinc porphyrin moiety. A characteristic signal was observed at 6.91 ppm in the  $^1\text{H}$  NMR spectrum (Figure S3). The signal was assigned as  $\beta_5$ , which was significantly shielded by the facing porphyrin. On the other hand, **4Zn<sub>2</sub>** gave only **E** dimer, in which protons of  $\beta_5$ – $\beta_8$  were not very

affected by the other facing porphyrin (Figure S5). The UV-vis spectral patterns of the **S** and **E** dimers in chloroform (Figure S7) are similar in the range of 650–850 nm to those of **1Zn<sub>2</sub>** in chloroform and 2-propanol shown in Figure 3a and 3b, respectively. Thus, the longest wavelength peak of **S** dimer is observed at 749 nm, which is relatively longer than that of **E** dimer. The compared analysis using discrete **S** and **E** dimers strongly supports that **1Zn<sub>2</sub>** formed in 2-propanol is **S** polymers.

Almost similar UV-Vis spectral changes were observed for **2Zn<sub>2</sub>** in chloroform and in 2-propanol (Figure S8). Unfortunately,  $^1\text{H}$  NMR spectral analyses of the **S** polymers of both **1Zn<sub>2</sub>** and **2Zn<sub>2</sub>** were difficult because of aggregation tendencies. Crystallization for single crystal X-ray diffraction analysis was also a failure; it gave only amorphous precipitates.

Macroscopic structural analysis of **S** polymers was then carried out by atomic force microscopy (AFM) and gel permeation chromatography (GPC). Samples for AFM analysis were prepared using a flow microreactor, in which a solution of **1Zn<sub>2</sub>** in chloroform and pure 2-propanol (1:10) were mixed to give  $1.2 \times 10^{-5}$  M solution of **1Zn<sub>2</sub>**. The mixed flow solution was directly deposited on a mica substrate, followed by rotation on a spin coater. The UV-Vis spectrum of the mixed solution was the same as the spectrum shown in Figure 3b. In a close-up image (Figure 5), long entangled wires were observed. The heights of the wires measured at the parts that were not overlaid were 2–3 nm, which is consistent with height estimated from a molecular model of **S** polymer (Figure 6).

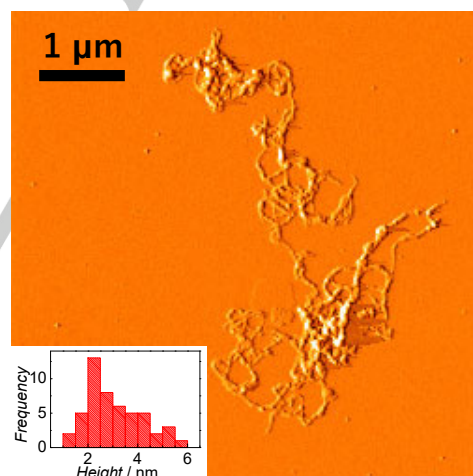


**Figure 5.** An AFM image of **1Zn<sub>2</sub>** on mica deposited as a mixed solution of chloroform and 2-propanol (1:10) ( $12 \mu\text{mol/L}$ ); a phase image; Long wires seem to be entangled or overlaid. (inset) a histogram of heights of the wires.

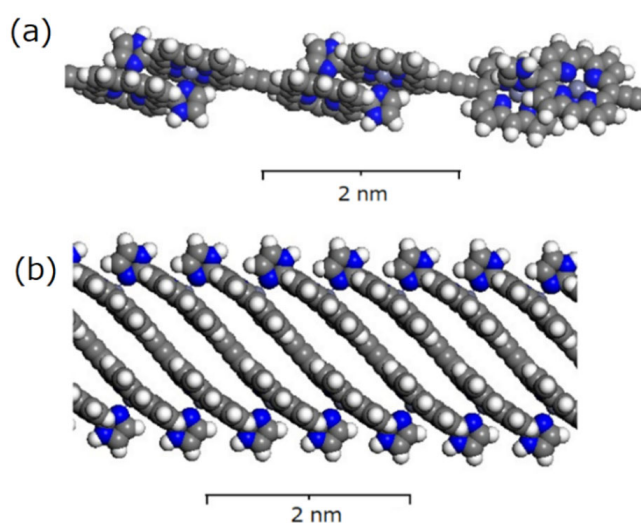


**Figure 6.** Molecular models of parts of (a) **E** and (b) **S** polymers. (blue: nitrogen, gray: carbon, white: hydrogen, light gray: zinc) Estimated thicknesses of the polymers are 1.2 nm for **E**, and 2.3 nm for **S** polymers, respectively. Side chains were omitted for clarity.

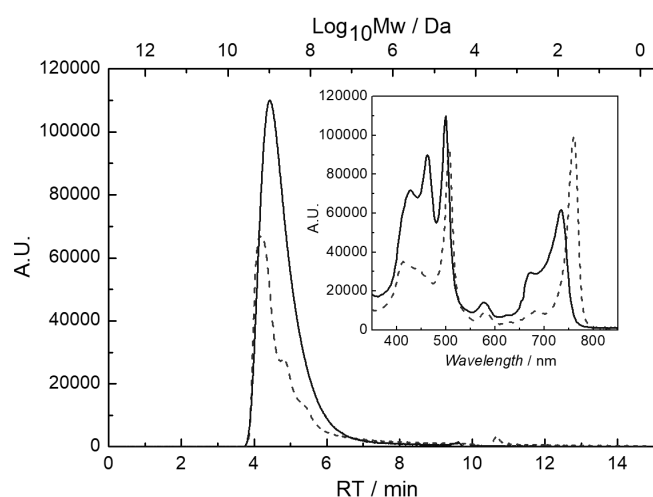


**Figure 7.** GPC charts of  $2\text{Zn}_2$  on a PLgel 20  $\mu\text{m}$  mixed-A column (Polymer laboratories, exclusion limit 40,000 kDa) with use of a mixture of  $\text{CHCl}_3$  : DME= 90:10 ((a) solid line) and 50:50 ((b) broken line) as eluents. (inset) the absorption spectra at RT 4.43 min of (a) (solid line), and at RT 4.19 min of (b) (broken line).

GPC analysis was also performed, using a polystyrene-base GPC column (Polymer Laboratories, PLgel 20  $\mu\text{m}$  MIXED-A, exclusion limit 40,000 kDa). As **S** polymers tend to aggregate to give insoluble precipitates, **E** polymers dissolved in chloroform were injected. **E** to **S** transformation was carried out through a flow pathway by changing eluent compositions of chloroform and 1,2-dimethoxyethane (DME). Here, DME affects **E** polymers to give **S** polymers. To estimate molecular sizes from elution volumes, calibration plots were prepared using standard

polystyrenes (16,100 kDa, 1,860 kDa, 70 kDa) (Figure S9). Figure 7 shows GPC charts of  $2\text{Zn}_2$  (monitored at 500 nm) after using two different solvent compositions. The top scale of the figure indicates the logarithm of the molecular weights prepared from the calibration plots. The structures at each peak were determined from UV-Vis spectra, using a photodiode-array detector (see inset in Figure 7). In  $\text{CHCl}_3$ :DME = 90:10, only **E** polymers were observed for both  $1\text{Zn}_2$  (solid line in Figure S10) and  $2\text{Zn}_2$  (solid line in Figure 7), whereas in  $\text{CHCl}_3$ :DME = 70:30 and 50:50, **S** polymers of  $1\text{Zn}_2$  and  $2\text{Zn}_2$  were observed (broken lines in Figures S10 and 7, respectively). The sizes of both **E** and **S** polymers are unexpectedly large, and they reached, or exceeded, the exclusion limit (40,000 kDa). Based on the results of UV-Vis spectral analysis compared with the related compounds and macroscopic structural analysis (using AFM and GPC), the samples prepared in 2-propanol or DME-rich solution were assigned as **S** polymers.

Surface areas of **E** and **S** polymers were estimated from molecular models, **E** 30mer and **S** 30mer, which were prepared using a molecular mechanics method, with a universal parameter (Figure S11). Their solvent accessible surface areas at 1.4  $\text{\AA}$  were calculated to be ca.  $2.5 \times 10^4$  and  $1.7 \times 10^4$   $\text{\AA}^2$ , respectively. Thus, the surface area of the **S** 30mer was reduced to approximately 70% of that of the **E** 30mer. This tendency is probably accelerated by elongation of polymer length, because intra- and intermolecular aggregation among **S** polymers occurs, as observed in the AFM image in Figure 5.

#### Thermodynamic Parameters in Binary Solvent Systems

To examine the thermodynamic behavior of the interconversion between **E** and **S** polymers, a mixed state of **E** and **S** polymers was prepared in a binary solvent system of 1,1,2,2-tetrachloroethane (TCE) and DME. It is noteworthy that only **E** or **S** polymers were observed in a TCE solution or a DME-rich solution, respectively. The mixed state of **E** and **S** polymers is a limited balance point, which can easily collapse when the solvent composition and/or concentration is changed.

Various temperature (VT)-UV-Vis spectra of  $2\text{Zn}_2$  ( $1.3 \times 10^{-5}$  M) were recorded in the temperature range 10–70 $^\circ\text{C}$  in a mixture of TCE and DME (60:40 vol/vol) (Figure 8a). The ratios of **E** and **S** polymers were determined from the change in intensity at 767 nm. From the **E**/**S** ratios at the various temperatures, the van't Hoff plots were prepared (Figure 8b). As the plots at 10 $^\circ\text{C}$  and 20 $^\circ\text{C}$  did not fit an approximation curve (probably because equilibrium was not reached), they were removed when preparing the final approximation curve. From the slope and the intercept,  $\Delta H = 29.2 \pm 2.9$  kJ/mol and  $\Delta S = 90.8 \pm 8.9$  J/mol/K were determined. Both the enthalpy and the entropy terms are positive, indicating that the transformation from **S** to **E** polymer is driven by entropy control, whereas the reverse process from **E** to **S** polymer is enthalpy controlled.



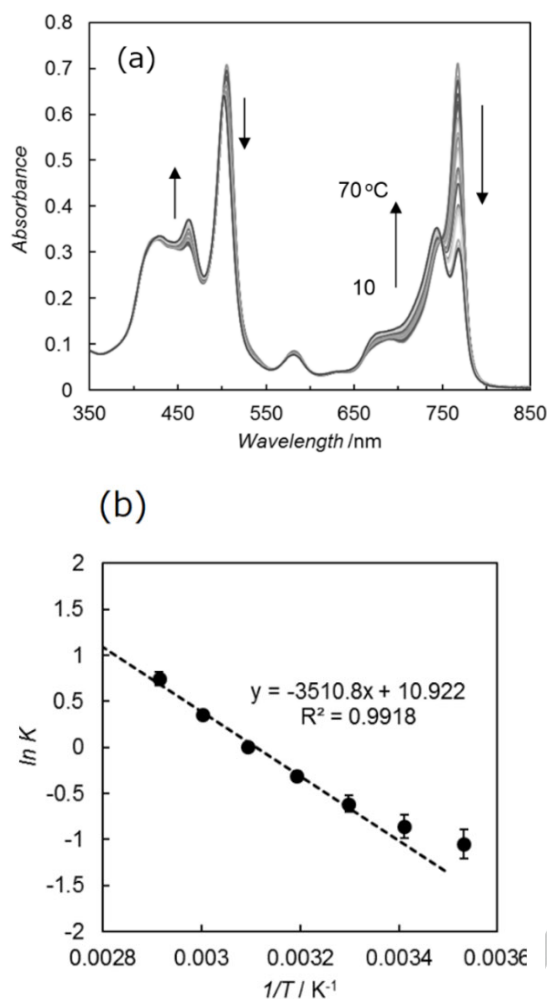


**Figure 8.** a) VT-UV-vis spectral changes of **2Zn<sub>2</sub>** in TCE : DME (60:40) from 10 to 70°C; Arrows indicate the transition from **S** to **E** polymers. b) van't Hoff plots of the transformation in Figure 7a.

In the transformation from **E** to **S** polymers, desolvation is considered to be accompanied. As the result, the entropy contributing to the solvent molecules increases, whereas the entropy contributing to the porphyrin moieties decreases due to loss of conformational freedom. On the other hand, large exothermic interaction among the porphyrins, such as the van der Waals interaction, is expected. Totally, the enthalpy term overcomes the entropy term, when transformation from **E** to **S** polymers proceeds. On the contrary, the conformational freedom of the porphyrin moieties drives the transformation of **S** polymers to **E** polymers, which have larger solvent-accessible surface areas and an easily rotating 1,3-butadiyne moiety, compared with corresponding **S** polymers. See Figures 6a and S11.

To estimate the rates of the interconversion, solvent-jump experiments were performed. When TCE was added to a solution of **S** polymers in DME containing 60 vol% TCE, the **S** polymers were immediately converted into **E** polymers. This was difficult to record on a conventional spectrometer. The opposite

conversion from **E** to **S** polymers also proceeded immediately, on the same time scale. No obvious transition states, such as monomers, were observed during the process. This result suggests that **E** polymers were destabilized in DME to give **S** polymers, whereas **S** polymers were destabilized in TCE to give **E** polymers. The transformations occur very rapidly.

#### Structures of **1Zn<sub>2</sub>** and **2Zn<sub>2</sub>** in Various Solvents

The above alternative formation system of **E** and **S** polymers was applied to a solvation/desolvation indicator in solution. Initially, 58 common solvents were examined. The method is quite simple and responsive. Thus, an aliquot (30  $\mu$ L) of chloroform solution of **1Zn<sub>2</sub>** or **2Zn<sub>2</sub>** was added to 3 mL of assessed solvent in a cuvette at 25°C. The concentration of the resulting solution should be  $< 3 \times 10^{-6}$  M to prevent heavy precipitation by interwire aggregation. Here, solutions were adjusted to a final concentration of  $2.5 \times 10^{-6}$  M. After stirring for 1 min, the mixture was recorded on a UV-Vis spectrometer. The results indicate that most of the solvents gave only **E** or **S** polymers exclusively, suggesting that, in these solvents, the Gibbs free energy change between **E** and **S** polymers is large. In some solvents, a mixture of **E** and **S** polymers was initially observed, but after 24 h there was conversion to **S** polymers. This is indicated as "**E+S**  $\rightarrow$  **S**". This phenomenon is similar to that observed in a binary solvent system of TCE and DME. It suggests that the Gibbs free energy change between **E** and **S** polymers is relatively small and that some activation energy is required. Only some solvents (trichloroethylene, 1-bromopropane, anisole, and 2,6-lutidine) gave mixtures of **E** and **S** polymers, for both, or either of **1Zn<sub>2</sub>** and **2Zn<sub>2</sub>**, even after 24 h, indicating that the Gibbs free energy change between **E** and **S** polymers is very close. Some solvents gave dissociated monomer **M**, or a mixture of **M** and **S**, or a mixture of **M** and **E**. These solvents have a coordination ability for the zinc porphyrin parts, as competitors for the imidazolyl moiety. The results are listed in Table S1 as "**S**", "**E**", "**E**  $\rightarrow$  **E+S**", "**E+S**  $\rightarrow$  **S**", "**E+S**", "**M**", "**M+S**", or "**M+E**" (asterisks in the table denote major components). The formation of **E** polymers indicates that the solvent that is used has a high solvation ability towards the porphyrin derivatives. The solvation interaction must be a van der Waals interaction between the solvent and the porphyrin, and it acts competitively to overcome the van der Waals interactions between porphyrin derivatives. Solvents, which initially or permanently gave a mixture of **E** and **S** polymers, have medium solvation ability. No, or less, solvent-solute interaction between the porphyrin derivatives is expected for the solvents; they immediately gave **S** polymers only.

In Table S1, solvents are listed in the order of one of the empirical solvent scales ( $\pi^*$ )<sup>[14]</sup>, determined experimentally from solvatochromism. Another solvent scale ( $E_{T(30)}$ )<sup>[6b]</sup>, and the macroscopic physical parameters<sup>[6b, c]</sup>, refractive index  $n$  and dielectric constant  $\epsilon$ , induced polarizability and dispersion interaction functions  $(n^2-1)/(n^2+1)$ <sup>[6c]</sup>, and dipolar-dipolar interaction function  $(\epsilon-1)/(\epsilon+1) - (n^2-1)/(n^2+1)$ <sup>[6c]</sup> are also listed for each solvent. Available Hildebrand solubility parameters<sup>[15]</sup> were listed in Table S2.

**S** polymers tend to form in solvents with relatively small  $\pi^*$  values, such as nonpolar solvents (hexane, toluene, carbon tetrachloride, and tetrachloroethylene) and some nonaromatic polar solvents having large dipole–dipole interaction values (alcohols, aliphatic nitriles, ketones, amides, and nitroalkanes). In these solvents, the porphyrin derivatives exclude the solvents. These phenomena are often called as solvophobic effects<sup>[16]</sup> and can be explained qualitatively; the sum of the solute–solute<sup>[17]</sup> and the solvent–solvent<sup>[18]</sup> interactions are greater than the solute–solvent interaction in the above solvents. As empirically known, close values of Hildebrand solubility parameters ( $\delta_c$ ,  $c$ :cohesive energy density) between solute and solvent tend to be soluble to each other<sup>[15]</sup>. The porphyrin derivatives are solvated in  $\text{CHCl}_3$  ( $\delta_c$  19.0) and  $\text{CH}_2\text{Cl}_2$  ( $\delta_c$  19.8) well, but they are desolvated in some solvents even having the close  $\delta$  values to those of  $\text{CHCl}_3$  and  $\text{CH}_2\text{Cl}_2$ , such as ethyl acetate ( $\delta_c$  18.6) and tetrachloroethylene ( $\delta_c$  19.0) (Table S2). These results suggest that the contribution of solvent–solvent interaction in the solvophobic effect is smaller than that of the solute–solute interaction.

Although tetrahydrofuran (THF) and trichloroethylene are solvents that have relatively small  $\pi^*$  values, they gave **E** polymers, or partially gave **E** polymers, suggesting that they have solvation ability. Solvents with higher  $\pi^*$  values frequently give **E** polymers, and differences between **1Zn<sub>2</sub>** and **2Zn<sub>2</sub>** were observed, which suggests the existence of a substituent effect on the porphyrin frames. In solvents with relatively large  $\pi^*$  values, no further relationship was observed between the  $\pi^*$  scale and the solvation ability to give **E** polymers. Furthermore, no relationship was observed between the tendency to give **E** polymers, and other solvent scales and macroscopic physical parameters in Table S1.

When the peak maxima of the Soret band in both **E** and **S** polymers were plotted against the optical dielectric constant,  $2(n^2-1)/(2n^2+1)$ , linear relationships were observed for both polymers (Figure S12). The linear relationships suggest a solvatochromism, which is applicable to molecules having large transition dipole moments, such as porphyrins<sup>[19]</sup>. The greater slope observed in **E** polymers indicates that they are better solvated than **S** polymers. This is reasonable, because **E** polymers have a larger solvent-accessible surface. It is noteworthy that the two lines of the **E** and **S** polymers exist independently in the same region of the x-axis. Our findings indicate that it is difficult to predict whether **E** or **S** polymers are produced from macroscopic physical parameters. Solvatochromic phenomena are observed, including many interactions and bulk solvent effects, whereas the present solvent indicator system can discriminate van der Waals interactions between solvent and solute from bulk solvent effects.

### Structure-Based Classification of Solvents

To clarify the interactions of the solvation, we carried out structure-based analysis of the solvents. For this analysis, several additional solvents and liquid compounds were examined on the solvation/desolvation indicator using **1Zn<sub>2</sub>** and **2Zn<sub>2</sub>**. A total of 67 liquid materials were classified into the following solvent groups (see Table 1): monohalogenated

nonaromatic compounds, multichlorinated nonaromatic compounds, bis(monochloromethyl) compounds, benzene and methylated benzenes, halogenated benzenes, functionalized benzenes, ethers, other nonaromatic compounds, and potentially coordinating solvents having lone pairs. Structures of the liquid compounds and all spectra are shown in Figures 9 and S13-1~S13-9, respectively (presented in the order of the solvent groups).

From the classification, four types of solvating solvents appeared to give **E** polymers: (1) nonaromatic hydrohalocarbons, (2) bidentate bis(monochloromethyl) compounds, (3) halobenzenes, except fluorobenzenes, and (4) some nonhalogenated functionalized benzenes. One remarkable result emerged was that THF was a good solvation solvent in the case of nonaromatic ethers.

Type (1) compounds (Nos 3, 4, 6, 7, and 11): Since no substitution effect between **1Zn<sub>2</sub>** and **2Zn<sub>2</sub>** was observed, except in the case of 1-bromopropane, hydrohalocarbons directly interact with the porphyrin frames. The strength of solvation of haloalkanes increases in the order  $\text{RCl} < \text{RBr} < \text{RI}$ , which correlates to larger atomic and electronic polarization on the halogen atoms. Monochloroalkanes (Nos 1, 2, and 5) do not solvate the porphyrins very effectively; however, multichlorination on a carbon atom is effective towards increasing their solvation ability, e.g.,  $\text{CH}_2\text{Cl}_2$  and  $\text{CHCl}_3$ . At least one hydrogen atom is necessary in a solvent molecule. In fact,  $\text{CCl}_4$  and  $\text{CCl}_2=\text{CCl}_2$  do not solvate porphyrins (Nos 8 and 10). It is possible that the hydrogen atoms play a role in the generation of their molecular dipole and/or  $\text{CH}-\pi$  interaction between the acidic hydrogen and  $\pi$ -electrons on the porphyrins.

Tsuzuki has reported on the importance of the hydrogen atom in chlorohydrocarbons in the dispersion interaction with benzene on the basis of high-level ab initio calculations<sup>[20]</sup>.

Type (2) compounds (Nos 12–17): Although monochloromethylalkanes have poor solvation ability (Nos 1, 2, and 5), bidentate bis(chloromethyl) compounds can solvate porphyrins effectively. The results suggest that two monochloromethyl moieties in a molecule interact with porphyrins cooperatively, like bidentate ligands in chelate complexes. Such a bidentate interaction must be entropically favored. The lengths of the alkylenyl moieties affect the solvation ability. Thus, 1,4- and 1,6-dichloroalkanes gave **E** polymers for both **1Zn<sub>2</sub>** and **2Zn<sub>2</sub>** (Nos 13 and 15), whereas shorter 1,2- and longer 1,8-dichloroalkanes gave a mixture of **E** and **S** polymers for **1Zn<sub>2</sub>** (No. 12), and **S** polymers for **2Zn<sub>2</sub>** (No. 16), respectively. These results suggest that the bite angles of the two interaction sites are important for the van der Waals interaction. In the case of 1,8-dichlorooctane, secondary interaction between the alkylenyl group and the undecyl moieties on **1Zn<sub>2</sub>** assists the solvation. Interestingly, when oxygen atoms were introduced into the alkylenyl groups, the selectivity of the solvation was reversed to **2Zn<sub>2</sub>** (Nos 14 and 17). The selectivity suggests repulsive interaction between the ether moieties in the chloroethyl ethers and the undecyl moieties on **1Zn<sub>2</sub>**. The side chains on the porphyrin derivatives control the solvation through the secondary interaction.

**Table 1.** Structures of  $1Zn_2$  and  $2Zn_2$  in various solvents.

no.	solvent	$1Zn_2$	$2Zn_2$
--- Monohalogenated non-aromatic compounds ---			
1	1-chloropropane	S	S
2	1-chlorobutane	S	S
3	1-bromopropane	S*+E	S
4	iodomethane	E	E
5	2-chloropropane	S	S
--- Multichlorinated non-aromatic compounds ---			
6	dichloromethane	E	E
7	chloroform	E	E
8	carbon tetrachloride	S	S
9	trichloroethylene	E→S+E*	S*+E
10	tetrachloroethylene	S	S
11	1,1,2,2-tetrachloroethane	E	E
--- Bis(monochloromethyl) compounds ---			
12	1,2-dichloroethane	E*+S→E+S*	E
13	1,4-dichlorobutane	E	E
14	bis(2-chloroethyl)ether	S	E
15	1,6-dichlorohexane	E	E
16	1,8-dichlorooctane	E	S
17	1,2-bis(2-chloroethoxy)ethane	S	E
--- Benzene and methylated benzenes ---			
18	benzene	S	S
19	toluene	S	S
20	p-xylene	S	S
21	mesitylene	S	S
--- Halogenated benzenes ---			
22	fluorobenzene	S	S
23	1,2-difluorobenzene	S	S*+E
24	1,3-difluorobenzene	S	S
25	chlorobenzene	E	E
26	1,2-dichlorobenzene	E	E
27	bromobenzene	E	E
28	mesityl bromide	E	S
29	1-bromo-2,4,6-triisopropylbenzene	S	S
30	iodobenzene	E	E
--- Functionalized benzenes ---			
31	ethyl benzoate	S*+E	S*+E
32	benzonitrile	E→S+E	E
33	acetophenone	S+E*→S*+E	E
34	nitrobenzene	E	E
35	N-methylformanilide	S	E
36	phenylacetone	S	E
37	anisole	S*+E	E
38	diphenyl ether	S	S
39	dibenzyl ether	S	S+E*→S
40	m-cresol	M+S*	M
--- Ethers ---			
41	diethyl ether	S	S
42	1,2-dimethoxyethane	S	S
43	Tetrahydrofuran	E	E
44	Tetrahydropyran	E	S
45	1,4-dioxane	S	M+S*
--- Other non-aromatic compounds ---			
46	Methanol	S	S
47	Ethanol	S	S
48	2-propanol	S	S
49	n-butanol	S	S
50	t-butanol	S	S
51	pentane	S	S
52	hexane	S	S
53	heptane	S	S
54	cyclohexane	S	S
55	methylcyclohexane	S	S
56	ethyl acetate	S	S
57	acetonitrile	S	S
58	butyronitrile	S	S
59	acetone	S	S
60	2-butanone	S	S
61	nitromethane	S	S
--- Potentially coordinating solvent having lone pair ---			
62	N,N-dimethylformamide	S	S+E*→S
63	N,N-dimethylacetamide	S	E*+M
64	dimethyl sulfoxide	S	S+M*
65	N,N-diisopropylethylamine	S	S
66	pyridine	M	M
67	2,6-lutidine	S+E*→S*+E	S+E*→S

E: Extended, S: Stacked, M: Monomer, Asterisk (\*): major component.

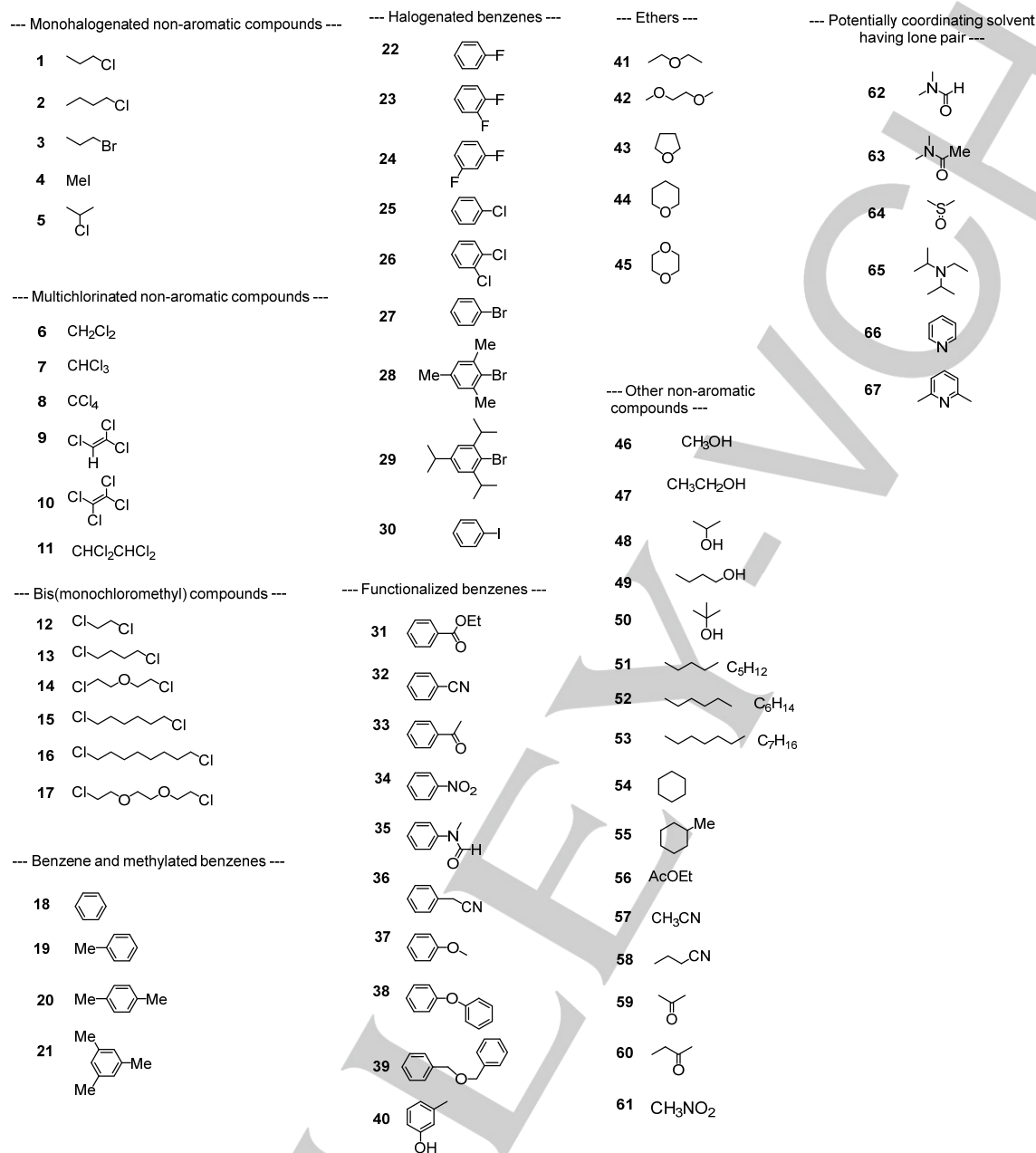


Figure 9. Structures of solvents and liquid compounds in Table 1.

The series of results recorded using bis(monochloromethyl) compounds suggests that the interaction between chloromethyl groups and porphyrin is specific and directional. An anisotropic model of solvents should be considered in the van der Waals interaction<sup>[21]</sup>.

Type (3) compounds (Nos 25–27, and 30): Except for fluorobenzenes, the halobenzenes (chloro-, bromo-, and iodobenzene) effectively solvate porphyrins. Because monochlorobenzene solvates porphyrins more effectively than monochloroalkanes, cooperative interaction between the

halogen and benzene parts in the halobenzene and the porphyrin moiety must exist. Introduction of three methyl or three 2-propyl groups on the bromobenzenes decreased the solvation ability (Nos 28 and 29). The results also suggest that the solvation interaction of halobenzene is specific, and correlates to the accessible distance and orientation. The interaction is probably related to halogen bonding observed in the cases of halobenzenes having electron-deficient substituents, such as fluoroiodobenzenes<sup>[22]</sup>. However, since simple chloro-, bromo-, and iodobenzenes can interact with the porphyrins here, a



further theoretical approach<sup>[23]</sup> is required. Reasons for the low solvation of fluorobenzenes (Nos 22–24) are probably its relatively low polarizability compared with that of other halobenzenes and the strong solvent–solvent interactions among the fluorobenzene molecules based on intermolecular H–F hydrogen bonding.

Type (4) compounds (Nos 31–37): Nonhalogenated functionalized benzenes that have strong electron withdrawing groups, such as nitrobenzene, benzonitrile, and acetophenone, also solvate porphyrins (Nos 32, 33, and 34). *N*-Methylformanilide, phenylacetonitrile, and anisole gave **E** polymers only in the case of **2Zn<sub>2</sub>** (Nos 35–37), indicating the effect of secondary interaction between the functional groups and the oligoether parts in the porphyrins. As similar aliphatic compounds (nitromethane, alkylnitriles, and alkylketones) did not solvate the porphyrins at all (Nos 57–61), it is the benzene parts that are considered essential for solvation of nonhalogenated compounds with the porphyrins. Aromatic stacking interactions may contribute the solvation<sup>[24]</sup>.

A very interesting result was that only THF solvates both porphyrin derivatives **1Zn<sub>2</sub>** and **2Zn<sub>2</sub>** (No. 43). The interaction mechanism is unclear, but two externally posted lone pairs on the oxygen atom can weakly coordinate with the zinc ion. The weak coordination may drive both **1Zn<sub>2</sub>** and **2Zn<sub>2</sub>** to their respective **E** polymers. Although the use of cyclic tetrahydropyran results in only **1Zn<sub>2</sub>** giving **E** polymers, nonaromatic acyclic ethers never gave **E** polymers for **1Zn<sub>2</sub>** and **2Zn<sub>2</sub>**.

Potentially coordinating solvents (Nos 62–67): *N,N*-dimethylacetamide and dimethyl sulfoxide gave a mixture of **E+M** and **S+M**, respectively, but only in the case of **2Zn<sub>2</sub>**. These results suggest that these solvents can weakly coordinate to the zinc ion with the assistance of a secondary interaction on the substituents. Pyridine (No. 66) has a strong coordination ability, to give monomers of both **1Zn<sub>2</sub>** and **2Zn<sub>2</sub>** perfectly, but 2,6-dimethylpyridine (No. 67), whose coordination ability is suppressed by the substitution, gives predominantly **S** polymers, which suggests that van der Waals interaction between porphyrin and pyridine frames is weak. The two effects, van der Waals interaction and coordination ability, seem to be independent.

As described in the former section, although  $\text{CHCl}_3$ ,  $\text{CH}_2\text{Cl}_2$ , ethyl acetate, and tetrachloroethylene have comparable Hildebrand solubility parameters ( $\delta$ ),  $\text{CHCl}_3$  and  $\text{CH}_2\text{Cl}_2$  gave **E** polymers, whereas ethyl acetate and tetrachloroethylene gave **S** polymers. Since their cohesive energy density values ( $\delta^2$ ) are close, each solvent–solvent interaction is comparable. Therefore, difference between  $\text{CHCl}_3$  and tetrachloroethylene is that  $\text{CHCl}_3$ , and also other “good” solvents, make the van der Waals interaction among the porphyrins (solute–solute interaction) weaken by their solvation. In other words, the “good” solvents to give **E** polymers are competitive against the van der Waals interaction among the porphyrins. It is interesting that coordination interaction of solvent to zinc ion seems to be independent on the van der Waals interaction.

The formation of **E** or **S** polymers occurs in the balance between the sum of solvent–solvent and solute–solute

interactions, and solvent–solute interaction. Therefore, the method described is considered an experimental system to evaluate many-body interactions. It is generally difficult to solve many-body interactions theoretically. In solution chemistry, therefore, computer-assisted molecular dynamic simulations have been examined to realize many-body interactions<sup>[25]</sup>. The present system will be useful as a model of many-body interactions.

A comparison of the substituent effects on **1Zn<sub>2</sub>** and **2Zn<sub>2</sub>** enabled clarification of the secondary interactions in the van der Waals interaction. In particular, the discovery of several functional benzenes as interactive molecules with the porphyrin derivatives is remarkable. These functional benzenes include nitrobenzene, benzonitrile, acetophenone, *N*-methylformanilide, phenylacetonitrile, and anisole. Our findings reveal that the system that we have described not only is a solvation/desolvation indicator but also becomes a probe to detect specific van der Waals interactions of benzene derivatives with porphyrin derivatives.

## Conclusions

We have accomplished the construction of molecular indicators to estimate both the solvation and desolvation ability of solvents towards the neutral nonpolar porphyrin derivatives. The method is very simple, like a litmus test, and it can be carried out using a conventional UV-Vis spectrometer.

The solvation observed here is based predominantly on van der Waals interaction between solvent and solute of large  $\pi$ -conjugated molecules. Thus, this method can discriminately monitor the van der Waals interaction, whereas most physicochemical phenomena such as solvatochromism include other interactions and bulk solvent effects.

A comparison of the substituent effects on the solutes enabled clarification of the secondary interactions in the van der Waals interaction. In the series of assessments, bischloromethyl compounds (which can interact with the solutes in a bidentate manner) and functional benzenes (which can interact with the porphyrin frames with assistance of secondary interactions with the substituents) now enter the arena as good partners for the porphyrins. The discovery indicates that the system is not only a solvation/desolvation indicator but it also becomes a probe to detect specific van der Waals interactions of functionalized molecules with porphyrin derivatives. As substituent groups on the porphyrin frames can potentially be replaced, various secondary interactions assisting van der Waals interaction can be surveyed. Therefore, the indicator system should contribute to the solution chemistry of molecules and materials, and to supramolecular chemistry interactions among hetero components.

## Conflicts of interest

There are no conflicts to declare.

## Experimental Section

**Absorption spectra in various solvents.** An aliquot (30  $\mu\text{L}$ ) of chloroform solution of **1Zn<sub>2</sub>** ( $3.5 \times 10^{-4}$  M) or **2Zn<sub>2</sub>** ( $3.8 \times 10^{-4}$  M) was added to 3 mL of assessed solvent in a cuvette at 25 °C. The concentration of the resulting solution were adjusted to a final concentration of  $2.5 \times 10^{-6}$  M. After stirring for 1 min, the mixture was recorded on a UV-Vis spectrometer.

**Experiments to determine the thermodynamic parameters ( $\Delta G$ ,  $\Delta H$ ,  $\Delta S$ ).** The solution of **2Zn<sub>2</sub>** ( $1.3 \times 10^{-5}$  M) heated to 70 °C in a mixed solvent of TCE and DME (6:4 v/v) was cooled to 10 °C. After reaching an equilibrium state at 10 °C, the temperature of the solution was gradually increased until reaching a target temperature for the measurement of UV-vis absorption spectrum. The molar ratios between the stacked and extended forms were calculated from the absorbance at 767 nm by assuming that the spectrum at 25 °C in TCE and DME (1.4:1 v/v) corresponded to that of the 100% stacked form and the spectrum at 25 °C in TCE and DME (1.8:1 v/v) corresponded to that of the 0% stacked form. From van't Hoff plots using the molar ratios between the stacked and extended forms, the  $\Delta H$  and  $\Delta S$  were calculated.

**Keywords:** van der Waals interaction • solvation • desolvation • porphyrin • supramolecular polymer

- [1] a) C. Reichardt, in *Solvents and Solvent Effects in Organic Chemistry*, Wiley-VCH Verlag GmbH & Co. KGaA, **2004**, pp. 93-145; b) R. Chakrabarty, P. S. Mukherjee, P. J. Stang, *Chem. Rev.* **2011**, *111*, 6810-6918.
- [2] a) G. A. Breault, C. A. Hunter, P. C. Mayers, *J. Am. Chem. Soc.* **1998**, *120*, 3402-3410; b) A. Tsuda, H. Hu, R. Tanaka, T. Aida, *Angew. Chem. Int. Ed.* **2005**, *44*, 4884-4888; c) T. Yamada, Y. Nagata, M. Sugimoto, *Chem. Commun.* **2010**, *46*, 4914-4916; d) S. Paliwal, S. Geib, C. S. Wilcox, *J. Am. Chem. Soc.* **1994**, *116*, 4497-4498.
- [3] Q. Cheng, S. Debnath, L. O'Neill, T. G. Hedderman, E. Gregan, H. J. Byrne, *J. Phys. Chem. C* **2010**, *114*, 4857-4863.
- [4] a) F. A. Carey, Sundberg, Richard J., in *Advanced Organic Chemistry Part A: Structure and Mechanisms*, Springer, **2007**, pp. 614-615; b) F. A. Carey, Sundberg, Richard J., in *Advanced Organic Chemistry Part A: Structure and Mechanisms*, Springer, **2007**, pp. 366-368.
- [5] a) C. Reichardt, in *Solvents and Solvent Effects in Organic Chemistry*, Wiley-VCH Verlag GmbH & Co. KGaA, **2004**, pp. 147-328; b) M. B. S. Jerry March, in *March's Advanced Organic Chemistry 6th edition*, 2007, Wiley Interscience, John Wiley & Sons, **2007**, pp. 501-504.
- [6] a) C. Reichardt, in *Solvents and Solvent Effects in Organic Chemistry*, Wiley-VCH Verlag GmbH & Co. KGaA, **2004**, pp. 329-388; b) C. Reichardt, in *Solvents and Solvent Effects in Organic Chemistry*, Wiley-VCH Verlag GmbH & Co. KGaA, **2004**, pp. 389-469; c) J.-L. M. A. a. R. Notari, *Pure Appl. Chem.* **1999**, *71*, 645-718.
- [7] L. Yang, J. B. Brazier, T. A. Hubbard, D. M. Rogers, S. L. Cockroft, *Angew. Chem. Int. Ed.* **2016**, *55*, 912-916.
- [8] a) Y. Tobe, N. Utsumi, K. Kawabata, A. Nagano, K. Adachi, S. Araki, M. Sonoda, K. Hirose, K. Naemura, *J. Am. Chem. Soc.* **2002**, *124*, 5350-5364; b) D. Zhao, J. S. Moore, *Chem. Commun.* **2003**, 807-818; c) Z. Chen, A. Lohr, C. R. Saha-Moller, F. Wurthner, *Chem. Soc. Rev.* **2009**, *38*, 564-584.
- [9] F. Biedermann, H.-J. Schneider, *Chem. Rev.* **2016**, *116*, 5216-5300.
- [10] a) A. Satake, J. Tanihara, Y. Kobuke, *Inorg. Chem.* **2007**, *46*, 9700-9707; b) A. Satake, T. Sugimura, Y. Kobuke, *J. Porphyrins Phthalocyanines* **2009**, *13*, 326-335.
- [11] A. Satake, M. Fujita, Y. Kurimoto, Y. Kobuke, *Chem. Commun.* **2009**, 1231-1233.
- [12] H. L. Anderson, *Inorg. Chem.* **1994**, *33*, 972-981.
- [13] a) M. U. Winters, J. Kämbart, M. Eng, C. J. Wilson, H. L. Anderson, B. Albinsson, *J. Phys. Chem. C* **2007**, *111*, 7192-7199; b) J. Kämbart, M. Gilbert, J. K. Sprafke, H. L. Anderson, B. Albinsson, *J. Phys. Chem. C* **2012**, *116*, 19630-19635.
- [14] C. Laurence, P. Nicolet, M. T. Dalati, J.-L. M. Abboud, R. Notario, *J. Phys. Chem.* **1994**, *98*, 5807-5816.
- [15] A. F. M. Barton, *Chem. Rev.* **1975**, *75*, 731-753.
- [16] L. Yang, C. Adam, S. L. Cockroft, *J. Am. Chem. Soc.* **2015**, *137*, 10084-10087.
- [17] a) C. A. Hunter, J. K. M. Sanders, *J. Am. Chem. Soc.* **1990**, *112*, 5525-5534; b) C. A. Hunter, M. N. Meah, J. K. M. Sanders, *J. Am. Chem. Soc.* **1990**, *112*, 5773-5780.
- [18] L. Yang, C. Adam, G. S. Nichol, S. L. Cockroft, *Nat. Chem.* **2013**, *5*, 1006.
- [19] T. H. Tran-Thi, J. F. Lipskier, P. Maillard, M. Momenteau, J. M. Lopez-Castillo, J. P. Jay-Gerin, *J. Phys. Chem.* **1992**, *96*, 1073-1082.
- [20] S. Tsuzuki, K. Honda, T. Uchimaru, M. Mikami, A. Fujii, *J. Phys. Chem. A* **2006**, *110*, 10163-10168.
- [21] a) A. Eilmes, *Theor. Chem. Acc.* **2014**, *133*, 1538; b) P. T. Van Duijnen, T. L. Netzel, *J. Phys. Chem. A* **2006**, *110*, 2204-2213.
- [22] a) H. Wang, W. Wang, W. J. Jin, *Chem. Rev.* **2016**, *116*, 5072-5104; b) G. Cavallo, P. Metrangolo, R. Milani, T. Pilati, A. Priimagi, G. Resnati, G. Terraneo, *Chem. Rev.* **2016**, *116*, 2478-2601.
- [23] S. Tsuzuki, T. Uchimaru, A. Wakisaka, T. Ono, *J. Phys. Chem. A* **2016**, *120*, 7020-7029.
- [24] a) C. A. Hunter, K. R. Lawson, J. Perkins, C. J. Urch, *J. Chem. Soc., Perkin Trans. 2* **2001**, 651-669; b) J. Hwang, B. E. Dial, P. Li, M. E. Kozik, M. D. Smith, K. D. Shimizu, *Chem. Sci.* **2015**, *6*, 4358-4364; c) J. Hwang, P. Li, W. R. Carroll, M. D. Smith, P. J. Pellechia, K. D. Shimizu, *J. Am. Chem. Soc.* **2014**, *136*, 14060-14067.
- [25] a) M. B. Oviedo, B. M. Wong, *J. Chem. Theory Comput.* **2016**, *12*, 1862-1871; b) J. O. Sindt, P. J. Camp, *J. Chem. Phys.* **2015**, *143*, 024501.

## Entry for the Table of Contents (Please choose one layout)

Layout 2:

## FULL PAPER

**E (extended) polymers**  
Coordination isomers

**"Bad" solvents:** benzene, toluene, alkanes, alkylchlorides, alcohols, alkylnitriles, alkylketones, ethers, nitromethane

**"Good" solvents:** CH<sub>2</sub>Cl<sub>2</sub>, CHCl<sub>3</sub>, C<sub>6</sub>H<sub>5</sub>Cl, C<sub>6</sub>H<sub>5</sub>Br, C<sub>6</sub>H<sub>5</sub>I, C<sub>6</sub>H<sub>5</sub>NO<sub>2</sub>, (C<sub>6</sub>H<sub>5</sub>CN) etc.

**S (stacked) polymers**  
UV-Vis spectral change

67 solvents were tested.

Akiharu Satake,\* Yuki Suzuki, Motonobu Sugimoto, Tatsumi Shimazaki, Hidekazu Ishii, Yusuke Kuramochi

Page No. – Page No.

**A Solvation/Desolvation Indicator based on van der Waals Interactions between Solvent and Porphyrins**

Molecular indicators to assess van der Waals interaction between solvent and porphyrins have been developed. Van der Waals interactions are weak, but important, interactions in nature. However, their discriminate observation in solution has been difficult, because they tend to be obscured by other strong interactions and bulk solvent effects. The procedure is very simple, like a litmus test.